J. Sustain. Metall. (2016) 2:248–256
DOI 10.1007/s40831-016-0052-x

RESEARCH ARTICLE

Synthesis of Diverse $LiNi_xMn_yCo_zO_2$ Cathode Materials from Lithium Ion Battery Recovery Stream

Qina Sa[1] · Eric Gratz[1] · Joseph A. Heelan[1] · Sijia Ma[1] · Diran Apelian[1] · Yan Wang[1]

Published online: 4 April 2016

Abstract Currently, a large amount of spent lithium ion batteries is being landfilled in many countries every year; in order to recover and reuse critical materials, a low-cost and a high-efficiency lithium ion battery recovery process was developed at Worcester Polytechnic Institute. This process recovers valuable metal elements such as Ni, Mn, Co in the form of $LiNi_xMn_yCo_zO_2$ cathode materials, where x, y, and z can be tailored. Other elements such as Cu and steel are also recovered. In this work, it was confirmed that high performance $Ni_{1/3}Mn_{1/3}Co_{1/3}(OH)_2$, $Ni_{0.5}Mn_{0.3}Co_{0.2}(OH)_2$, $Ni_{0.6}Mn_{0.2}Co_{0.2}(OH)_2$ precursors and $LiNi_{1/3}Mn_{1/3}Co_{1/3}O_2$, $LiNi_{0.5}Mn_{0.3}Co_{0.2}O_2$, $LiNi_{0.6}Mn_{0.2}Co_{0.2}O_2$ cathode materials can be synthesized from the leaching solutions of a lithium ion battery recovery stream. The precursors and cathodes were synthesized from a co-precipitation process and a solid-state sintering process, respectively. Electrochemical tests results demonstrated that all cathode materials synthesized from spent lithium ion battery recovery streams performed at a discharge capacity higher than 155 mAh/g at first cycle of 0.1C, and after 100 cycles at 0.5C, with over 80 % of the capacity retained.

Keywords Lithium ion battery recovery · Co-precipitation · Precursor · $LiNi_xMn_yCo_zO_2$

The contributing editor for this article was S. Kitamura.

✉ Yan Wang
yanwang@wpi.edu

[1] Department of Mechanical Engineering, Worcester Polytechnic Institute, 100 Institute Road, Worcester, MA 01609, USA

Introduction

The amount of plug-in electric vehicles (PEVs) in the world has reached over 500,000 units as of June 2014 [1]. This new trend in the car market indicates that demand for lithium ion batteries will be continuously growing. However, an increase in lithium ion batteries implies that there will be more battery waste in the near future. Currently, most spent lithium ion batteries are landfilled in many countries, which creates tremendous threat to the environment and human health [2]. Another fact is that lithium ion battery waste contains valuable metal elements such as Li, Ni, Co, Mn, and Cu. For these reasons, there have been many efforts to recycle lithium ion batteries [3–6].

Initially, lithium ion battery recyclers focused solely on cobalt as $LiCoO_2$ was the main cathode material in the market; the high price of cobalt also motivated recycling efforts [7–9]. Currently, lithium ion battery cathode materials have become more diverse and different transition metal compounds have entered the market in the past few years. The waste stream includes lithium ion batteries with different cathode chemistries. As a result, an efficient lithium ion battery recovery process should not target a single cathode chemistry. A "mixed cathode" recycling process was first proposed and developed [10, 11], by which certain amounts of lithium ion batteries with diverse cathode materials can be recovered together without battery sorting. Ni, Mn, Co, and Li metal elements existed in the leaching stream with varying molarities. The concentrations of these valuable metal elements can be determined by inductively coupled plasma optical emission spectrometry (ICP-OES) and adjusted by adding MSO_4 (M=Ni, Mn, Co) salts, so metal hydroxide precursors and cathodes with different Ni:Mn:Co molar ratios can be synthesized directly. The recovery efficiency of these three metal elements can reach up to 90 %.

In this work, the leaching solution from the recovery stream was utilized to synthesize diverse $LiNi_xMn_yCo_zO_2$ cathodes. The first product synthesized was $LiNi_{1/3}Mn_{1/3}Co_{1/3}O_2$, which has been described previously [12]. Subsequently, the molarities of transition metal elements were adjusted to 5:3:2 and 6:2:2 to obtain $LiNi_{0.5}Mn_{0.3}Co_{0.2}O_2$ and $LiNi_{0.6}Mn_{0.2}Co_{0.2}O_2$. Before the co-precipitation experiments, the leaching solution was examined by ICP-OES to verify that all impurity elements were below 50 ppm. The main impurity elements were Cu, Al, and Fe. Cu and Al derived from the current collectors of the anode and cathode; Fe from $LiFePO_4$ cathode material and steel casing. $Ni_xMn_yCo_z(OH)_2$ precursors were synthesized via the co-precipitation process, which has been reported [13–17]. The precursors were then mixed with Li_2CO_3 to obtain the corresponding $LiNi_xMn_yCo_zO_2$ cathodes. Uniform and nearly spherical morphologies were observed in all the synthesized $LiNi_xMn_yCo_zO_2$ cathodes. These materials also demonstrated excellent rate performance and cycle life results.

Experimental

Synthesis of $LiNi_xMn_yCo_zO_2$ Cathode Materials Using Leaching Solutions from Lithium Ion Battery Recovery Process

A novel lithium ion battery recovery process was developed in our laboratory and has been previously described [10, 11]. The recovery efficiencies of Ni^{2+}, Mn^{2+}, Co^{2+} were over 90 %. The leaching solution could be obtained at the end of the recovery process. The overall process is shown in Fig. 1. After the remaining capacity was discharged, the spent lithium ion batteries first went through a mechanical treatment, including shredding, magnetic separation of the steel, sieving, and density separation to collect the cathode powder, which is the most valuable part of the battery. The collected powder was leached by H_2SO_4 and H_2O_2 so the valence of Ni, Mn, and Co elements could be reduced to 2^+. This 2^+ valence is very critical for spherical shape formation [18]. The impurity elements such as Fe and Cu were removed by adjusting the pH of the solution. Ni, Mn, and Co elements co-exist in the leaching solution as the spent lithium ion battery cathodes were a random mixture of $LiCoO_2$, $LiNi_xMn_yCo_zO_2$, $LiFePO_4$, Li_2MnO_4, etc. The leaching solution was stored in a N_2 atmosphere to prevent the Mn^{2+} from oxidizing. Depending on the molar ratios of Ni:Mn:Co in different target cathode materials, the calculated amount of MSO_4 (M=Ni, Mn, Co) was added into the solution to achieve molarity ratios such as 1:1:1, 5:3:2, 6:2:2; the molarity was confirmed by ICP-OES. The molar ratio of Ni:Mn:Co in the solution can be adjusted to any values, indicating NMC cathode materials with diverse Ni:Mn:Co can be achieved with this leaching solution. Once the $Ni_xMn_yCo_z(OH)_2$ material is obtained, corresponding $LiNi_xMn_yCo_zO_2$ cathodes can be synthesized depending on the need.

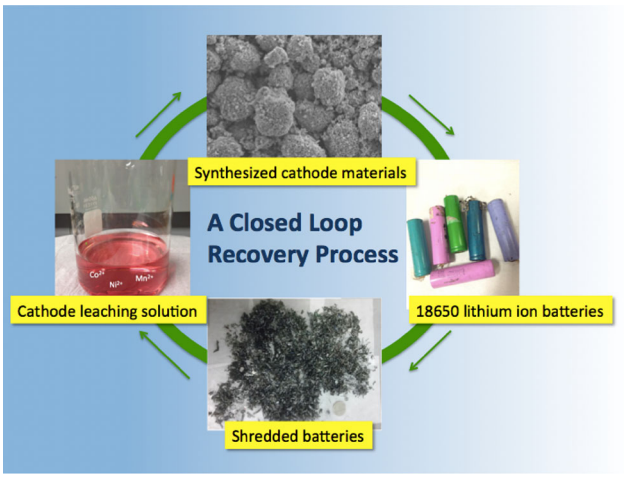

Fig. 1 Lithium ion battery recovery process developed at WPI-CR[3] center

$Ni_xMn_yCo_z(OH)_2$ precursors were synthesized via a co-precipitation process involving NaOH and $NH_3{\cdot}H_2O$ solutions. In this experiment, 200 ml of 1 M $NH_3{\cdot}H_2O$ was first put into the reactor and heated to 60 °C. Then 5 M $NH_3{\cdot}H_2O$ and 2 M MSO_4 solutions were pumped into the reactor at rates of 10 and 30 ml/h, respectively. 5 M NaOH was automatically added throughout the reaction by a pH controller using a peristaltic pump to stabilize the reaction at the desired pH values. The feeding time of MSO_4 and $NH_3{\cdot}H_2O$ was 2 h; the reaction was then continued for another 24 h. An overhead stirrer was utilized and the stirring speed was maintained at 500 rpm. The synthesized precursor was filtered and washed until the filtered solution's pH was 7; then the material was furnace dried at 110 °C for 12 h.

To synthesize $LiNi_xMn_yCo_zO_2$ cathodes, the $Ni_xCo_yCo_z(OH)_2$ precursor was thoroughly mixed with Li_2CO_3 by mortar and pestle. The ratio of Li:$Ni_xMn_yCo_z(OH)_2$ was 1.03 at.% for $LiNi_{1/3}Mn_{1/3}Co_{1/3}O_2$, 1.08 at.% for $LiNi_{0.5}Mn_{0.3}Co_{0.2}O_2$, and 1.10 at.% for $LiNi_{0.6}Mn_{0.2}Co_{0.2}O_2$. For $LiNi_{1/3}Mn_{1/3}Co_{1/3}O_2$, $LiNi_{0.5}Mn_{0.3}Co_{0.2}O_2$, and $LiNi_{0.6}Mn_{0.2}Co_{0.2}O_2$, the mixtures were heated to 900, 850, and 800 °C. respectively. These mixtures were heated in air for 12 h and both the heating rate and cooling rate were maintained at 2 °C/min.

Battery Assembling and Electrochemical Property Tests of Synthesized $LiNi_xMn_yCo_zO_2$ Cathodes

The lithium ion battery electrode was prepared from the mixture of 10 wt% polyvinylidene fluorides (PVDF) binder, 10 wt% conductive additive C65, and 80 wt%

synthesized $LiNi_xMn_yCo_zO_2$ cathode materials. The mixture was turned into slurry then cast onto an aluminum foil as the cathode. The electrode was furnace dried overnight at 60 °C. After the electrode was completely dry, a piece of 1/4 inch diameter electrode was punched from the whole piece and pressed to a thickness of 50 μm. The loading mass was 5 mg/cm^2. The electrochemical properties were tested with Swagelok cells assembled in an argon gas-filled glove box. The electrolyte was 1 M $LiPF_6$ dissolved in ethylene carbonate, dimethyl carbonate, and diethyl carbonate (EC + DMC + DEC, 1:1:1 in volume). Lithium metal served as the anode during the electrochemical test. All tests were conducted at room temperature.

Characterization

ICP-OES (Perkin Elmer Optical Emission Spectrometer, Optima 8000) was utilized to measure the concentrations of desired ions in solution. An X-ray diffraction (XRD) pattern was obtained from a diffractometer (PANalytical Empyrean Series 2 X-ray Diffraction System, with chromium Ka radiation, Cr target) by scanning the powder with a 2θ range of 20°–120° at a step size of 0.008° and scanning step time of 20 s. The operation voltage and current of XRD machine were 30 kV and 55 mA, respectively. HighScore Plus software was utilized to perform Rietveld refinements. The particle size and morphology were observed by scanning electron microscope (SEM) (JEOL JSM-7000F electron microscope). The electrochemical performance was examined by an Arbin electrochemical tester. The rate performance was tested at C/10, C/5, C/3, C/2, C, 2C. The cell was charged and discharged at 0.1C for three cycles before running a 0.5C cycle test. The cut off voltage was 4.3 V for charging and 2.7 V for discharging. 1C rate was calculated as 160 mAh/g.

Results and Discussion

Molar Ratio Adjustment of Ni:Mn:Co in Leaching Solution

The recycling process started from a mixture of spent lithium ion batteries with random composition without any sorting, signifying that the concentration of each element is not predictable and needs to be confirmed by ICP-OES. Also, to obtain different kinds of NMC precursors, the molar ratio of Ni:Mn:Co in the MSO_4 (M=Ni, Mn, Co) solution should be close to 1:1:1, 5:3:2, and 6:2:2, corresponding to the products of $Ni_{1/3}Mn_{1/3}Co_{1/3}(OH)_2$, $Ni_{0.5}Mn_{0.3}Co_{0.2}(OH)_2$, and $Ni_{0.6}Mn_{0.2}Co_{0.2}(OH)_2$. It has been reported that Mn^{2+} plays an important role in synthesizing spherical-shaped $Ni_{1/3}Mn_{1/3}Co_{1/3}(OH)_2$ particles [18]. Once Mn^{2+} is oxidized to Mn^{3+}, it will prevent the particles from forming spherical shapes and affect the co-precipitation reaction [18]. Therefore, after the solution is obtained by leaching cathode powders, bubbling the solution with N_2 for 15 min is necessary, and then the solution container should be sealed carefully to prevent Mn^{2+} from being oxidized.

Table 1 shows the concentration of each element in a freshly leached solution from our recovery process as well as the concentration after the molarity adjustment step. In this case, since other impurity elements such as Fe, Al, Cu were well removed and were below 50 ppm in the solution, they were not included in these results. The three batches of 200 ml solutions obtained by leaching cathode powders were collected after the mechanical separation and leaching portions of the recovery process were completed. The molarities of transition metal ions were detected by ICP-OES. Subsequently,calculated amounts of $CoSO_4{\cdot}7H_2O$, $NiSO_4{\cdot}6H_2O$, and $MnSO_4{\cdot}H_2O$ were added into batches of 200 mL each to obtain 1:1:1, 5:3:2, and 6:2:2 molar ratios of Ni:Mn:Co, followed by diluting the solution to 250 ml. The molar ratios of these Ni:Mn:Co were 1.03:1:0.97 [12], 5.04:3:1.96, and 5.98:2.00:2.01, which were confirmed by ICP-OES. The molar ratios of Ni: Mn: Co in every synthesized precursors were tested again, and found to be exactly the same as in the starting solutions. It should be noted that lithium ions from spent lithium ion batteries existed in the solution from the beginning of the leaching step to the end of co-precipitation process, and remained in the filtered solution after washing the precipitate with DI water. Lithium ions could not be precipitated out during the co-precipitation process because the pH and temperature of the solution was not suitable for lithium recovery. Lithium recovery will be discussed in future work.

Product 1: $LiNi_{1/3}Mn_{1/3}Co_{1/3}O_2$ Cathode

The first target product is $LiNi_{1/3}Mn_{1/3}Co_{1/3}O_2$ because it is one of the most commonly used cathode materials. The 1:1:1 molar ratio offers a good balance of safety, capacity, and reversibility. The details of the co-precipitation process

Table 1 Metal elements concentrations in freshly leached solution (concentration-1) [12] and molar ratio adjusted solutions (concentration 2 [12], 3 and 4)

	Co	Ni	Mn	Li
Concentration-1 (M)	0.37	0.12	0.07	1.07
Concentration-2 (M)	0.65	0.69	0.67	0.85
Concentration-3 (M)	1.08	0.6	0.39	0.85
Concentration-4 (M)	1.22	0.41	0.42	0.85

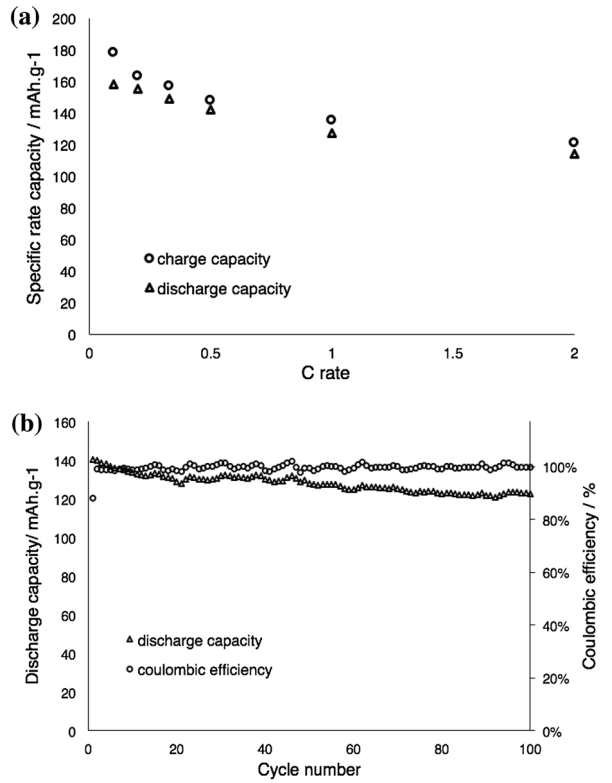

Fig. 2 Specific rate performance (**a**) and cycle life performance (**b**) of Product 1

and solid-state synthesis of the cathode materials were reported previously [12].

The rate capacity test results of $LiNi_{1/3}Mn_{1/3}Co_{1/3}O_2$ at C/10, C/5, C/3, C/2, C, and 2C are shown in Fig. 2a. It achieved a charge capacity of 178 mAh/g and discharge capacity of 158 mAh/g in the first 0.1C cycle with a coulombic efficiency of 89 %. The discharge capacities were 153, 149, 142, and 127 mAh/g at C/2, C/3, C/5, and 1C, respectively. At higher C rates of 2C, the discharge capacity continued to perform at an acceptable rate of 114 mAh/g, indicating the layered structure of cathode was stable at a higher current.

The capacity reversibility test was conducted at 0.5C with a cutoff voltage of 2.74.3 V (Fig. 2b). Over 85 % capacity was maintained after 50 cycles and the coulombic efficiency maintained a good performance of >98 %.

Product 2: $LiNi_{0.5}Mn_{0.3}Co_{0.2}O_2$ Cathode

Compared to $LiNi_{1/3}Mn_{1/3}Co_{1/3}O_2$, there is more Ni in the $LiNi_{0.5}Mn_{0.3}Co_{0.2}O_2$ compound. Also, during the co-precipitation reaction of $Ni_{0.5}Mn_{0.3}Co_{0.2}(OH)_2$, the pH value is slightly higher than that of $Ni_{1/3}Mn_{1/3}Co_{1/3}(OH)_2$ because of higher amounts of Ni [16].

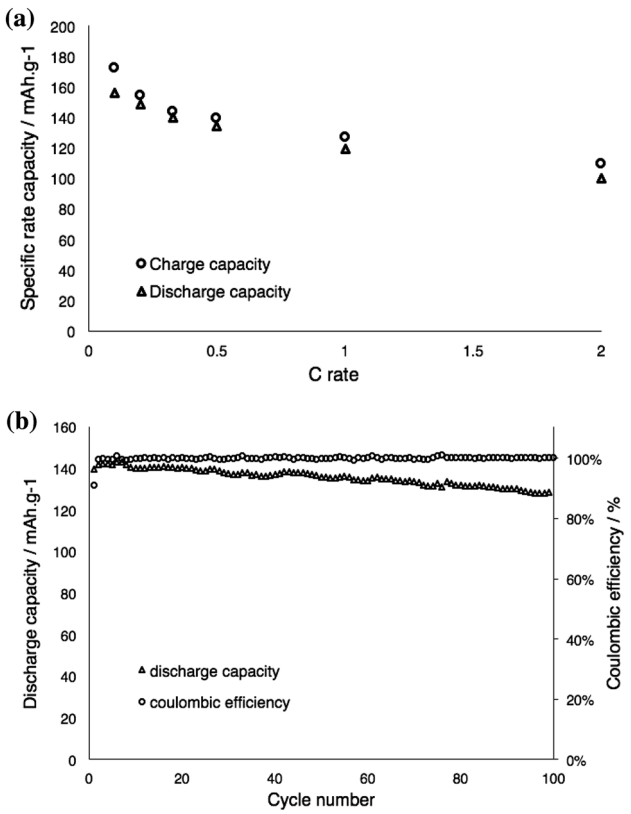

Fig. 3 Specific rate performance (**a**) and cycle life performance (**b**) of Product 2

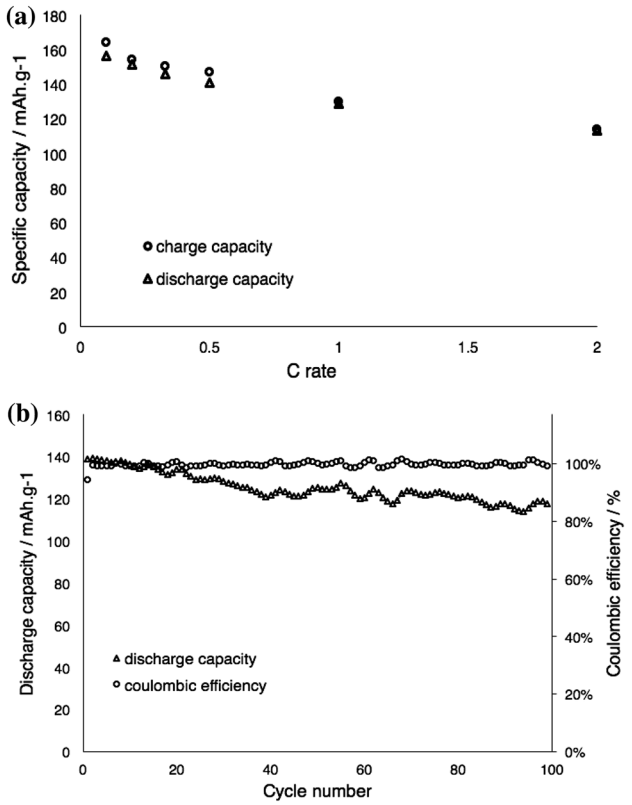

Fig. 4 Specific rate performance (**a**) and cycle life performance (**b**) of Product 3

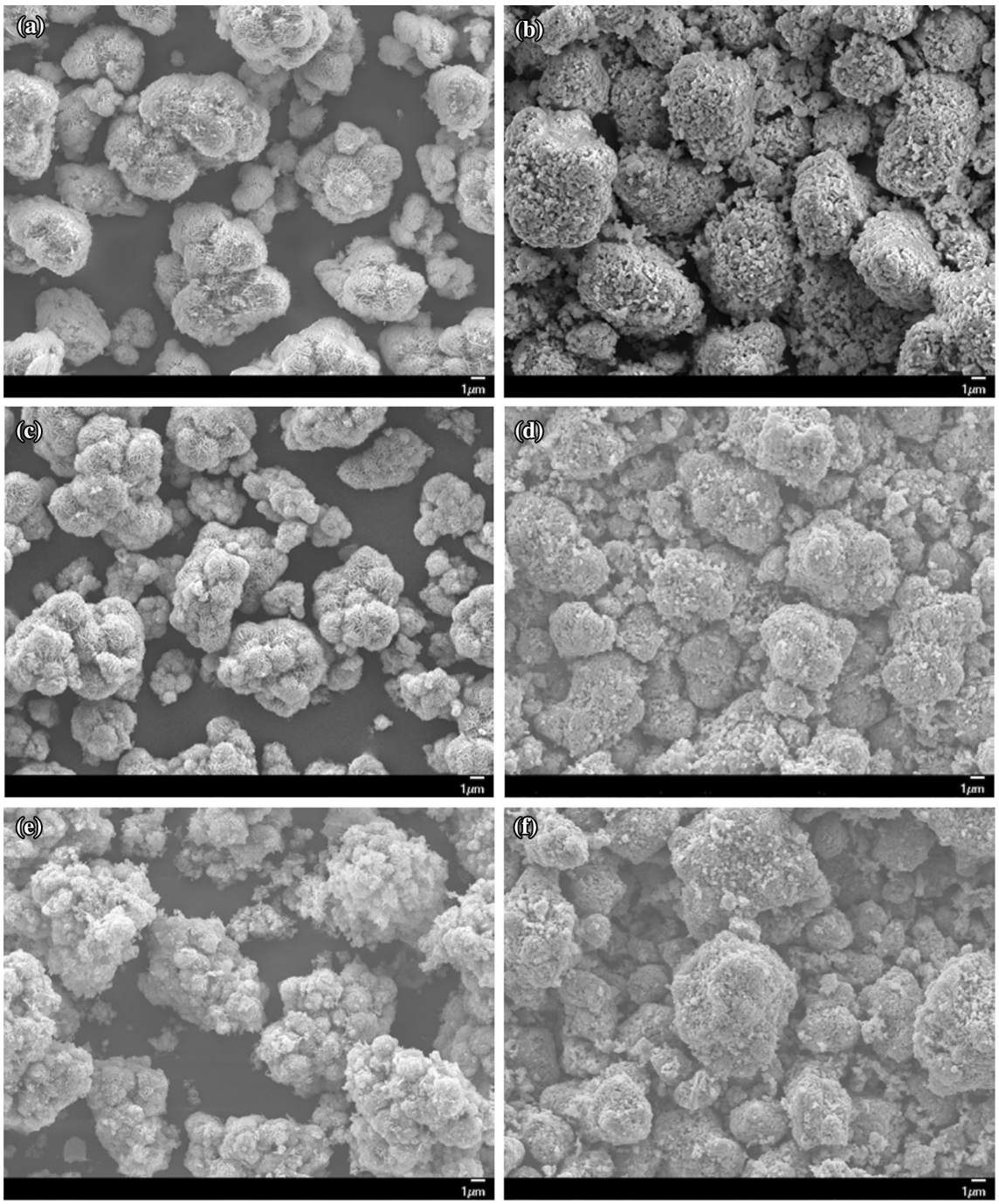

Fig. 5 Particle morphologies of synthesized precursors—$Ni_{1/3}Mn_{1/3}Co_{1/3}(OH)_2$ (**a**), $Ni_{0.5}Mn_{0.3}Co_{0.2}(OH)_2$ (**c**), and $Ni_{0.6}Mn_{0.2}Co_{0.2}(OH)_2$ (**e**), and their corresponding cathode materials (**b**, **d**, and **f**)

The electrochemical test results of $LiNi_{0.5}Mn_{0.3}Co_{0.2}O_2$ cathode are shown Fig. 3a, b. Similar to $LiNi_{1/3}Mn_{1/3}Co_{1/3}O_2$, C/10, C/5, C/3, C/2, C, and 2C rate capacity tests were carried out. The capacity reversibility was examined by cycling the battery at 0.5C for 100 cycles. The synthesized $LiNi_{0.5}Mn_{0.3}Co_{0.2}O_2$ from recycled materials performed quite well at rate capacities of 156, 148, 139, 134, 119, and 108 mAh/g at C/10, C/5, C/3, C/2, C, and 2C, respectively (Fig. 3a). After 100 cycles at 0.5C, over 87 % capacity had remained (Fig. 3b).

Product 3: $LiNi_{0.6}Mn_{0.2}Co_{0.2}O_2$ Cathode

After $LiNi_{1/3}Mn_{1/3}Co_{1/3}O_2$ and $LiNi_{0.5}Mn_{0.3}Co_{0.2}O_2$ were synthesized, the molar percentage of the Ni element was raised again to obtain $LiNi_{0.6}Mn_{0.2}Co_{0.2}O_2$. For the

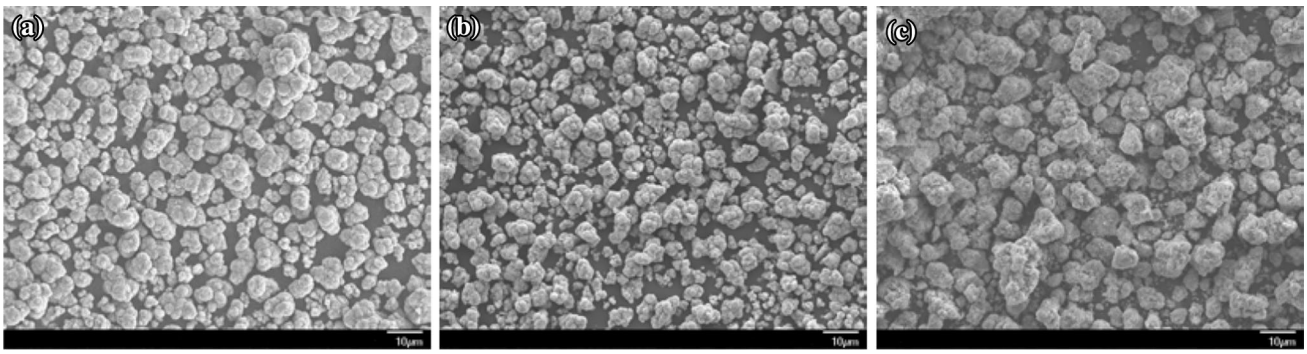

Fig. 6 Particle morphologies comparison of synthesized precursors—$Ni_{1/3}Mn_{1/3}Co_{1/3}(OH)_2$ (**a**), $Ni_{0.5}Mn_{0.3}Co_{0.2}(OH)_2$ (**b**), and $Ni_{0.6}Mn_{0.2}Co_{0.2}(OH)_2$ (**c**)

sintering process, $Ni_{0.6}Mn_{0.2}Co_{0.2}(OH)_2$ precursor was mixed with Li_2CO_3 at 800 °C, which is the lowest sintering temperature among the three products because of the higher concentration of Ni.

The specific rate capacity and capacity retention evaluation results for $LiNi_{0.6}Mn_{0.2}Co_{0.2}O_2$ are shown in Fig. 4. At C/10, a discharge capacity of 158mAh/g was obtained. And 152, 146, 141, 130, and 113 mAh/g discharge capacities were achieved at C/5, C/3, C/2, C, and 2C, respectively (Fig. 4). $LiNi_{0.6}Mn_{0.2}Co_{0.2}O_2$ also shows good capacity reversibility. After 100 cycles of charging and discharging at 0.5C, 85 % of the original capacity had remained (Fig. 4b).

Comparison and Discussion of Three Precursors and Cathode Products

As the molar ratio of Ni increases, the properties of precursors and cathode materials change. The first difference that can be clearly observed is the color of freshly synthesized precursors. $Ni_{1/3}Mn_{1/3}Co_{1/3}(OH)_2$ is a light pink color powder, $Ni_{0.5}Mn_{0.3}Co_{0.2}(OH)_2$ and $Ni_{0.6}Mn_{0.2}Co_{0.2}(OH)_2$ are light green. Co^{2+} ions contribute to the pink color, Ni^{2+} ions contribute to the green/blue color. Since $LiNi_{0.5}Mn_{0.3}Co_{0.2}O_2$ has less Co and more Ni, its color is light green. When the precursors are dried at elevated temperatures, they are easily oxidized and their color undergoes changes from yellow to dark brown and finally black at the end.

Figure 5 shows the scanning electron micrographs of synthesized $Ni_xMn_yCo_z(OH)_2$ precursors and $LiNi_xMn_yCo_zO_2$ cathodes. The morphologies of $LiNi_xMn_yCo_zO_2$ are dependent on the starting $Ni_xMn_yCo_z(OH)_2$ morphology. The synthesized $LiNi_{1/3}Mn_{1/3}Co_{1/3}O_2$ particles have more spherical shapes compared to $LiNi_{0.5}Mn_{0.3}Co_{0.2}O_2$ and $LiNi_{0.6}Mn_{0.2}Co_{0.2}O_2$ particles because $Ni_{1/3}Mn_{1/3}Co_{1/3}(OH)_2$ precursor had the most spherical morphology.

The precursor particles had a uniform particle size of 8–10 μm and they were nearly spherical, among which $Ni_{1/3}Mn_{1/3}Co_{1/3}(OH)_2$ (Fig. 5a) and $LiNi_{1/3}Mn_{1/3}Co_{1/3}O_2$ (Fig. 5b) have the most smooth spherical shapes. In the precursor particles, the crystal forms a thin and sharp feature, and such morphology leads to a long and slim cylindrical shape in the $LiNi_xMn_yCo_zO_2$ primary particles after sintering with Li_2CO_3. It was observed from the SEM analyses that the cathode particles were dense and well crystallized; moreover, the spherical shapes of the precursors were retained. Figure 5c, e shows the $Ni_{0.5}Mn_{0.3}Co_{0.2}(OH)_2$ and $Ni_{0.6}Mn_{0.2}Co_{0.2}(OH)_2$ morphologies, respectively. Figure 5d, f shows the corresponding cathode morphologies. Figure 6 visually compares the three different precursors. When the Ni amount is raised to 50 and 60 %, the spherical shape in the precursors is not as smooth as the product with even Ni: Mn: Co molar ratios. This is likely because of using the same reaction parameters (except pH value) for the precursors with different metal molar ratios. During the co-precipitation processes of $Ni_{0.5}Mn_{0.3}Co_{0.2}(OH)_2$ and $Ni_{0.6}Mn_{0.2}Co_{0.2}(OH)_2$ precursors, the feeding rate ratios of MSO_4/ammonia water were the same as that used with $Ni_{1/3}Mn_{1/3}Co_{1/3}(OH)_2$ precipitation. To achieve better morphologies, the feeding rates could be adjusted as the Ni:Mn:Co molar ratio changes in the MSO_4 solution as the morphologies of the co-precipitated products are highly affected by the feeding rate ratio of MSO_4/ammonia water [19]. Also, in $Ni_{1/3}Mn_{1/3}Co_{1/3}(OH)_2$, the three metal elements are evenly distributed and tend to produce uniform spherical shapes.

To allow the particles to grow to the desired sizes for the three precursors, the co-precipitation pH values of the synthesis processes were adjusted. It has been reported that in $Ni(OH)_2$ precipitation process, the particles grows at a pH of 11.4 or less. When involving Mn and Co, a lower pH is required [16]. As the molar ratio of Ni was decreased and the Mn and Co concentration were increased, the pH value

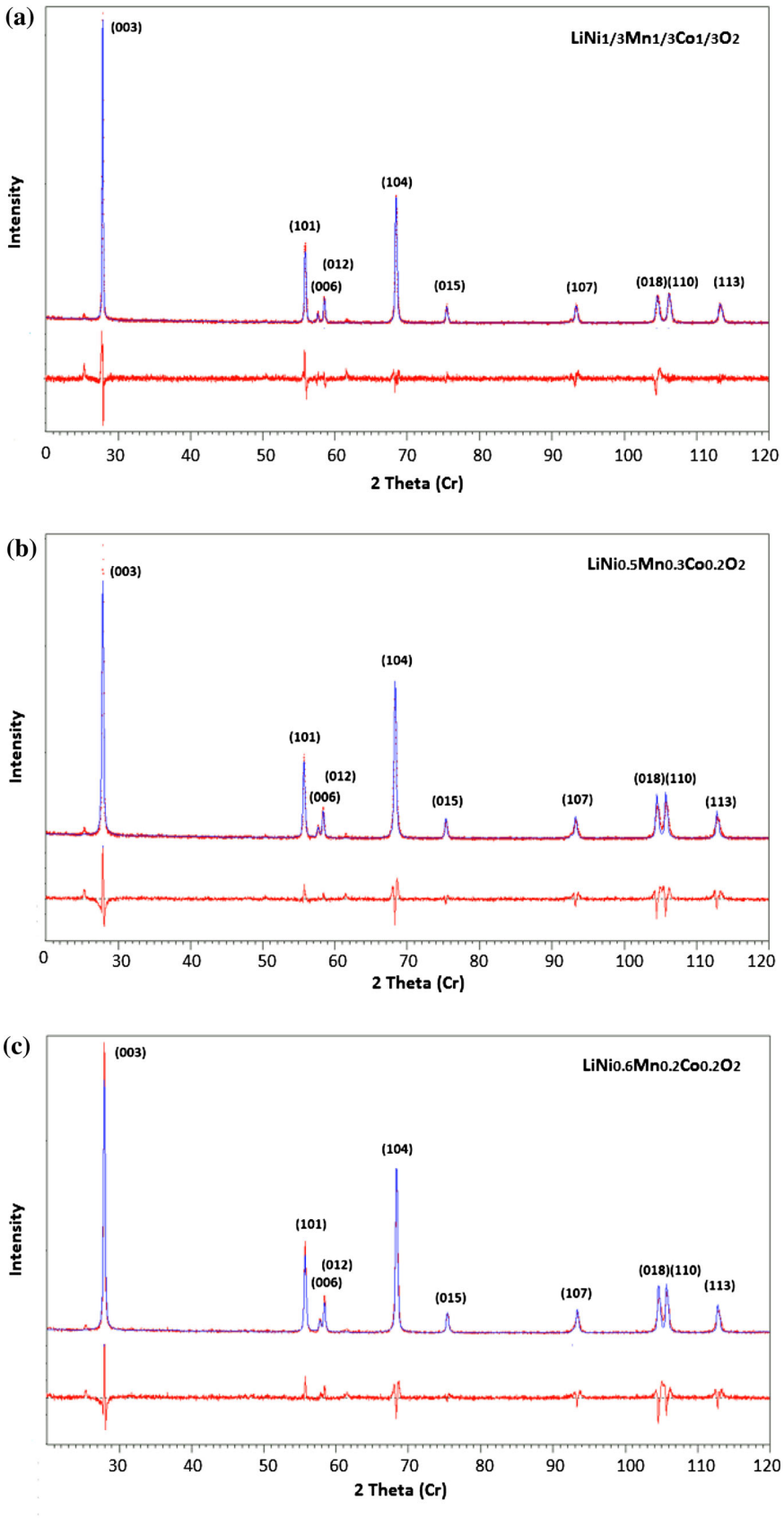

Fig. 7 XRD refinement patterns of synthesized cathode materials—$LiNi_{1/3}Mn_{1/3}Co_{1/3}O_2$ (**a**), $LiNi_{0.5}Mn_{0.3}Co_{0.2}O_2$ (**b**), and $LiNi_{0.6}Mn_{0.2}Co_{0.2}O_2$ (**c**)

Table 2 XRD refinement results of $LiNi_{1/3}Mn_{1/3}Co_{1/3}O_2$ [12], $LiNi_{0.5}Mn_{0.3}Co_{0.2}O_2$, and $LiNi_{0.6}Mn_{0.2}Co_{0.2}O_2$

	Lattice parameters		Reliability factors and scale factor			
	a (Å)	c (Å)	Rwp (%)	Rp (%)	Re (%)	s
$LiNi_{1/3}Mn_{1/3}Co_{1/3}O_2$	2.86442 (2)	14.2661 (1)	6.08	4.47	4.92	1.23
$LiNi_{0.5}Mn_{0.3}Co_{0.2}O_2$	2.87203 (2)	14.2476 (1)	5.87	3.98	2.91	2.02
$LiNi_{0.6}Mn_{0.2}Co_{0.2}O_2$	2.87313 (2)	14.2354 (1)	4.90	3.30	2.66	1.84

should be lowered. Ni appears to be coordinated with ammonia at a pH of 4–12, whereas Mn and Co coordinate at a pH of 6–10 [16]. In our experiments, the co-precipitation pH for $Ni_{1/3}Mn_{1/3}Co_{1/3}(OH)_2$ is 10, and for $Ni_{0.5}Mn_{0.3}Co_{0.2}(OH)_2$ and $Ni_{0.6}Mn_{0.2}Co_{0.2}(OH)_2$ the pH values are 10.2 and 11, respectively. And the precursor particles grew to a size range of 8–10 μm.

XRD refinement results of $LiNi_{1/3}Mn_{1/3}Co_{1/3}O_2$ [12], $LiNi_{0.5}Mn_{0.3}Co_{0.2}O_2$, and $LiNi_{0.6}Mn_{0.2}Co_{0.2}O_2$ are shown in Fig. 7 and Table 2. The XRD peaks look clear and sharp with a clean background in all three patterns, and show an α-$NaFeO_2$ structure with a space group of Rm. The peaks (006) and (012), (018) and (110) are separated distinctly, indicating the products are well crystalized and are pure. The refinement shows a good fit between calculated and synthesized NMC patterns. The ratios of cation and anion are: $c/a = 4.98$ [12], 4.96, and 4.95, showing that the appropriate layered structure was formed in the compound. The scale factor (s) values are all below or around 2, indicating that the fitting was good.

The electrochemical test results show that $LiNi_{1/3}Mn_{1/3}Co_{1/3}O_2$, $LiNi_{0.5}Mn_{0.3}Co_{0.2}O_2$, and $LiNi_{0.6}Mn_{0.2}Co_{0.2}O_2$ have excellent specific rate capacities. All three synthesized cathode materials show the expected capacity retention. Compared to $LiNi_{1/3}Mn_{1/3}Co_{1/3}O_2$ and $LiNi_{0.5}Mn_{0.3}Co_{0.2}O_2$, $LiNi_{0.6}Mn_{0.2}Co_{0.2}O_2$ has slightly higher rate capacities due to the higher amount of Ni in the cathode. The electrochemical test result indicates that the cathodes synthesized by recycled materials can perform at acceptable capacities compared to those synthesized by commercial raw materials [19–21].

It should be noted that when the precursors were precipitated out from the MSO_4 solution generated from the lithium ion battery recovery process, a small amount of lithium element does exist in the precipitated product. According to the ICP-OES, the hydroxide precursor contains an atomic percentage of lithium within an acceptable level, lower than 0.4 % of any other metal elements. Thus, the effect of lithium element at the co-precipitation step is not an issue.

Conclusions

In the previously reported lithium ion battery recovery process, the molar ratio of Ni:Mn:Co could be controlled in a simple and flexible manner during the recovery process. In this work, the following diverse cathode products synthesized from the leaching solution were examined: $LiNi_{1/3}Mn_{1/3}Co_{1/3}O_2$, $LiNi_{0.5}Mn_{0.3}Co_{0.2}O_2$, and $LiNi_{0.6}Mn_{0.2}Co_{0.2}O_2$. By synthesizing new cathode materials that can be implemented into new batteries, the recycling process becomes a "closed loop" process raising the possibility of scaling it up and having a viable commercial battery recovery and reuse process. All the synthesized cathode particles showed uniform morphologies. Most importantly, the electrochemical properties of the $LiNi_xMn_yCo_zO_2$ synthesized through recovery and reuse (recycling) are acceptable compared to those synthesized from pure commercial product. Our future work will optimize the synthesis parameters of $LiNi_xMn_yCo_zO_2$ to further improve the quality of products.

Acknowledgments This work was financially supported by the National Science Foundation (NSF) under Grants 1230675, 1343439, and 1464535. We acknowledge the helpful discussions with the colleagues at WPI's Center for Resource Recovery and Recycling (CR3 an NSF I/UCRC).

References

1. Electric car use by country. http://en.wikipedia.org/wiki/Electric_car_use_by_country. Accessed 18 May 2015
2. Kang DHP, Chen M, Ogunseitan OA (2013) Potential environmental and human health impacts of rechargeable lithium batteries in electronic waste. Environ Sci Technol 47:5495–5503
3. Lain MJ (2001) Recycling of lithium ion cells and batteries. J Power Sources 97–98:736–738
4. Xu J, Thomas HR, Francis RW, Lum KR, Wang J, Liang B (2008) A review of processes and technologies for the recycling of lithium-ion secondary batteries. J Power Sources 177:512–527
5. Paulino JF, Busnardo NG, Afonso JC (2008) Recovery of valuable elements from spent Li-batteries. J Hazard Mater 150:843–849
6. Zhang P, Yokoyama T, Itabashi O, Suzuki TM, Inoue K (1998) Hydrometallurgical process for recovery of metal values from

spent lithium-ion secondary batteries. Hydrometallurgy 47:259–271
7. Contestabile M, Panero S, Scrosati B (2001) A laboratory-scale lithium-ion battery recycling process. J Power Sources 92:65–69
8. Shin SM, Kim NH, Sohn JS, Young DH, Kim YH (2005) Development of a metal recovery process from Li-ion battery wastes. Hydrometallurgy 79:172–181
9. Dorella G, Mansur MB (2007) A study of the separation of cobalt from spent Li-ion battery residues. J Power Sources 170:210–215
10. Zou H, Gratz E, Apelian D, Wang Y (2013) A novel method to recycle mixed cathode materials for lithium ion batteries. Green Chem 15:1183–1191
11. Gratz E, Sa Q, Apelian D, Wang Y (2014) A closed loop process for recycling spent lithium ion batteries. J Power Sources 262:255–262
12. Sa Q, Gratz E, He M, Lu W, Apelian D, Wang Y (2015) Synthesis of high performance $LiNi_{1/3}Mn_{1/3}Co_{1/3}O_2$ from lithium ion battery recovery stream. J Power Sources 282:140–145
13. Bommerl A, Dahn JR (2009) Synthesis of spherical and dense particles of the pure hydroxide phase $Ni_{1/3}Mn_{1/3}Co_{1/3}(OH)_2$. J Electrochem Soc 156(5):A362–A365
14. Lee MH, Kang YJ, Myung ST, Sun YK (2004) Synthetic optimization of $Li[Ni_{1/3}Co_{1/3}Mn_{1/3}]O_2$ via co-precipitation. Electrochim Acta 50:939–948
15. Liu Z, Yu A, Lee JY (1999) Synthesis and characterization of $LiNi_{1-x-y}Co_xMn_yO_2$ as the cathode materials of secondary lithium batteries. J Power Sources 81–82:416–419
16. Bommel A, Dahn J (2009) Analysis of the growth mechanism of coprecipitated spherical and dense nickel, manganese and cobalt-containing hydroxides in the presence of aqueous ammonia, contained. Chem Mater 21:1500–1503
17. Huang Y, Gao D, Lei G, Li Z, Su Y (2007) Synthesis and characterization of $Li(Ni_{1/3}Co_{1/3}Mn_{1/3})_{0.96}Si_{0.04}O_{1.96}F_{0.04}$ as a cathode material for lithium-ion battery. Mater Chem Phys 106:354–359
18. Zhao X, Zhou F, Dahn JR (2008) Phases formed in Al-doped $Ni_{1/3}Mn_{1/3}Co_{1/3}(OH)_2$ prepared by coprecipitation: formation of layered double hydroxide. J Electrochem Soc 155(9):A642–A647
19. Noh M, Cho J (2013) Optimized synthetic conditions of $LiNi_{0.5}Co_{0.2}Mn_{0.3}O_2$ cathode materials for high rate lithium batteries via co-precipitation method. J Electrochem Soc 160(1):A105–A111
20. Choi J, Manthiram A (2005) Role of chemical and structural stabilities on the electrochemical properties of layered $LiNi_{1/3}Mn_{1/3}Co_{1/3}O_2$ cathodes. J Electrochem Soc 152(9):A1714–A1718
21. Liang LW, Du K, Peng ZD, Cao YB, Hu GR (2014) Synthesis and electrochemical performance of $LiNi_{0.6}Co_{0.2}Mn_{0.2}O_2$ as a concentration-gradient cathode material for lithium batteries. Chin Chem Lett 25(6):883–886